ChemComm

Cite this: *Chem. Commun.*, 2012, **48**, 6654–6656

www.rsc.org/chemcomm

COMMUNICATION

One-step continuous synthesis of biocompatible gold nanorods for optical coherence tomography†

Víctor Sebastián,‡[a] Seung-Kon Lee,[a] Chao Zhou,[b] Martin F. Kraus,§[b] James G. Fujimoto*[b] and Klavs F. Jensen*[a]

Received 11th March 2012, Accepted 10th May 2012
DOI: 10.1039/c2cc32969g

We present a novel one-step flow process to synthesize biocompatible gold nanorods with tunable absorption and biocompatible surface ligands. Photothermal optical coherence tomography (OCT) of human breast tissue is successfully demonstrated using tailored gold nanorods designed to have strong absorption in the near-infrared range.

Gold nanorods (GNRs) have received much attention because of their potential in a wide variety of applications such as, biological imaging, sensors, surface enhanced Raman spectroscopy, drug delivery and photothermal therapy of cancer cells.[1,2] Seed mediated growth[3] in the presence of cetyltrimethyl ammonium bromide (CTABr) is the most widely used synthesis method to produce GNRs, comprising of at least two steps: synthesis of gold seeds, and then addition of the gold seeds to a CTABr/Au solution for growth of nanorods. CTABr is the structure-directing agent used to control nanorod shape, but CTABr-capped GNRs have been reported to be cytotoxic.[4] CTABr resulting from incomplete purification of the GNRs or desorption from the bound bilayer is toxic to cells as a detergent that adversely affect cell membranes.[5] Hence, proper purification of the GNRs is a key step for any *in vivo* work. Various approaches have been employed to retard CTABr desorption and to eliminate free CTABr molecules in nanoparticle solutions.[6] For example, the use of silver ions to assist in the growth of GNR is commonly used in seed-mediated approach. Silver ions are reduced to form monolayer or submonolayer of silver.[7] Fast silver deposition followed by strong CTABr binding inhibits gold growth on the sides of the rods leading to preferential anisotropic growth of gold at the ends.[8] Unfortunately, the presence of silver exacerbates the toxicity problem.[9] The seeded growth methods have also been reported to suffer from limited reproducibility perhaps attributable to the number of the steps involved.[10,11] Therefore, development of an alternative approach is necessary for the synthesis of biocompatible GNRs by means of a simple and versatile process.

In order to circumvent the toxicity and multistep issues associated with typical GNRs synthesis, we report a single-step process with lysine, a biocompatible amino acid, as the capping agent and without the presence of silver/CTABr.[12] Moreover, we have adapted the single-pot synthesis carried out in a batch reactor to a continuous flow process for improved synthesis control and reproducibility. Specifically, a solution of $Au(OH)_4^-$ at pH 10.3 is reduced in flow by sodium borohydride in presence of several amino acids: lysine, adenosine and alanine. The results demonstrate that rod-shape gold nanoparticles with strong absorption in the near infrared wavelength range (700–900 nm) can be prepared by tuning the lysine concentration. Selection of the optimal gold precursor species, pH and ligands are critical to the successful growth of nanorods.

Fig. 1 shows the absorption spectra of the growth products made with various molar ratios of lysine/gold (Lys/Au). Gold products synthesized with a Lys/Au molar ratio below 10 exhibit only transverse plasmon band (TPB). Upon further increase in the Lys/Au molar ratio, the TPB decreases in intensity and stays at 520 nm, becoming a shoulder of the longitudinal plasmon band (LPB), suggesting the conversion of nanospheres into nanorods. Finally, the LPB redshifts to the near infrared wavelength range with increases in width of the absorption. Transmission electron microscopy (TEM) images are in agreement with the optical data and shows that there is a transition from spherical-shape nanoparticles to nanorods as the Lys/Au ratio was increased ultimately resulting in nanorods with an aspect ratio of 4.5–5 at 180 Lys/Au (Fig. 2 and Fig. S1). Synthesis of GNRs was not feasible using other amino acids such as adenosine or alanine (Fig. S2a). In addition to the carboxylic acid functionality, lysine possesses two chemically distinct amino groups allowing both capping and bridging roles.[13] Lysine is thought to interact with the gold surface *via* the α-amine group, whereas the terminal amino group forms hydrogen bonds with the carboxylic acid group of surrounding lysine molecules, which promotes the gold nanoparticle linear assembly. The bridging role of lysine is

[a] *Department of Chemical Engineering, Massachusetts Institute of Technology, 77 Massachusetts Avenue, Cambridge, MA 02139, USA. E-mail: kfjensen@mit.edu*
[b] *Department of Electrical Engineering and Computer Science and Research Laboratory of Electronics, Massachusetts Institute of Technology, 77 Massachusetts Avenue, Cambridge, MA 02139, USA. E-mail: jgfuji@mit.edu*
† Electronic Supplementary Information (ESI) available. See DOI: 10.1039/c2cc32969g
‡ Present address: Universidad de Zaragoza, Departamento de Ingenieria Quimica, Instituto de Nanociencia de Aragon, C/Pedro Cerbuna 12, 50009 Zaragoza, Spain.
§ Present address: Pattern Recognition Lab, Graduate School in Advanced Optical Technologies (SAOT), University Erlangen-Nuremberg, 91054 Erlangen, Germany.

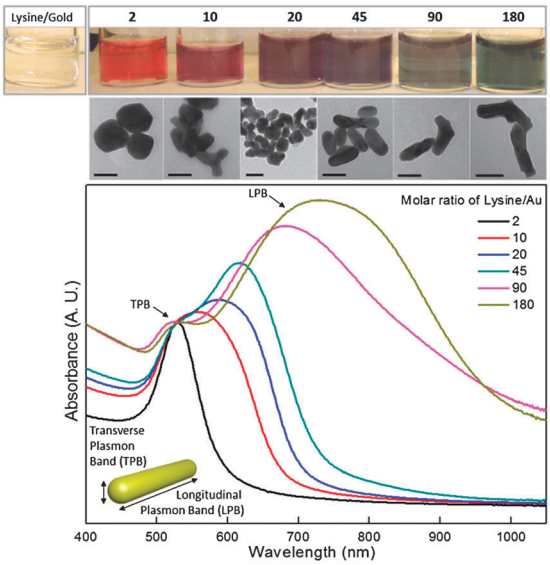

Fig. 1 Absorption spectra and TEM images of the gold nanorods (GNRs) grown with varying amounts of the lysine/gold precursor (Lys/Au) ratio. Various colors of the GNR solutions correspond to the absorption spectra of different Lys/Au ratios (top). Corresponding TEM images showing structural evolution (middle, also see Fig. S1). Scale bar is 30 nm.

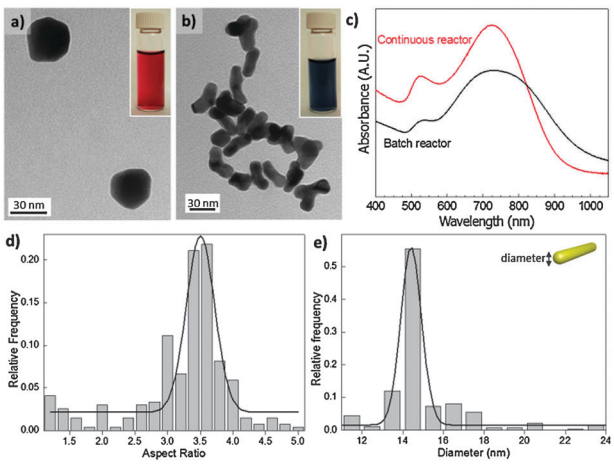

Fig. 2 TEM images and absorbance spectra of the Au nanostructures. (a) TEM image of Au nanostructures obtained at Lys/Au molar ratio of 2, in a batch reactor. (b) At molar ratio of 180, in a continuous flow reactor. Insets of (a) and (b) optical images from gold colloids obtained at different Lys/Au ratios. (c) Comparison of absorbance spectra from GNRs obtained in a batch reactor and continuous flow reactor (oxidant flow rate of 40 μL min^{-1} and reductant flow rate of 10 μL min^{-1}) with same Au/Lys molar ratio of 180. (d), (e) Statistical analysis of produced GNRs obtained in continuos flow: (d) aspect ratio and (e) diameter.

pH dependent and it is only effective at pH higher than its pK2 (8.5) (Fig. S2b). Above this pH, the amino terminal group is deprotonated, leading to capped gold nanoparticles with negative charged surfaces.[13] The unidirectional growth best minimizes the electrostatic repulsion forces, so as the concentration of lysine increases, the dual role of lysine capping/bridging promotes the growth of anisotropic gold nanostructures (Fig. 1, 2a and b). However, the directionality created by the lysine ligand is not perfect and some gold nanoparticles assembly in L or Y shapes, which would broaden the LPB. Moreover, poor mixing efficiency in the batch reactor tend to acerbate the broadening for fast reaction systems like the present one.

Slow and inhomogeneous mixing in batch systems leads to an uneven concentration distribution as well as a limitation in mass transfer.[14] Therefore, we adapted the batch synthesis to a continuous microfluidic flow process for a better control in the synthesis of GNR (Fig. S3). Moreover, being able to manipulate separate streams of the gold precursor and reducing agent enabled fast screening and optimization of the synthesis conditions. With application of the continuous reactor, optical properties of the resulting GNRs were significantly improved. Moreover, a high throughput was obtained as a result of the reduced characteristic time of the transport processes at micrometer length scale (Fig. S4). UV–VIS spectra show a better definition of the TPB and a narrower LPB absorption (Fig. 2c). From the statistical characterization, the aspect ratio of the resulting nanorods was about 3.5, with uniform diameter of 15 nm (Fig. 2d and e).

As shown in Fig. 3a and b, the lattice planes in the facets of the GNR continuously extended to form single crystals. These characterizations indicate a strong cross-linking interaction between the fused gold nanoparticles with the oriented attachment mechanism, where adjacent particles self-organize so that they share a common crystallographic orientation.[15] TEM images show that {111} plane is corresponding to the longitudinal axis of the GNRs. XRD data in Fig. 3c also support the TEM observations. Compared with the XRD spectra of the reference bulk gold, {111} orientations are significantly extended as much as 202%. It is known that the crystal orientations of short GNRs are dominated by {100} and {110} while long GNRs are dominated by {111} and {110}, when they are grown with CTABr.[16] However, for our short GNRs grown with lysine, {111} plane was significantly dominant over {100} and {110}. Crystallite size characterized by X-ray diffraction (XRD) are 14.1, 11.2, 13.4 nm for {111}, {100}, {110} plane, respectively.

Lysine is reported to promote the formation of gold linear chains at basic pH values,[13] but no LPB has been reported for these nanostructures. To demonstrate that not only the pH but also the gold species are important to obtain lysine capped GNRs, a synthesis of GNRs was carried out using fresh $AuCl_4^-$ solution at pH value of 10.3, where hydrolysis of Au–Cl does not occur completely.[17] Fig. S5 shows that the incomplete hydrolysis of Au–Cl bonds species promotes the

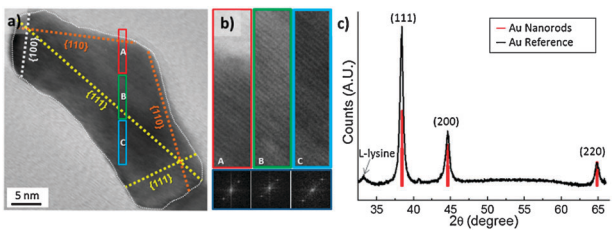

Fig. 3 HR-TEM and XRD analysis of the gold nanorods. (a), (b) HRTEM image with lattice orientations; {111}, {100} and {110}. (b) HRTEM images correspond to the colored boxes A, B and C in (a) presented in the left. Right images show Fourier transforms of A, B and C, respectively. (c) XRD spectrum from dried bulk GNRs (black). Spectrum from reference bulk gold (red). Small sub-peak at 33° is attributed to crystalline L-lysine from the residue.

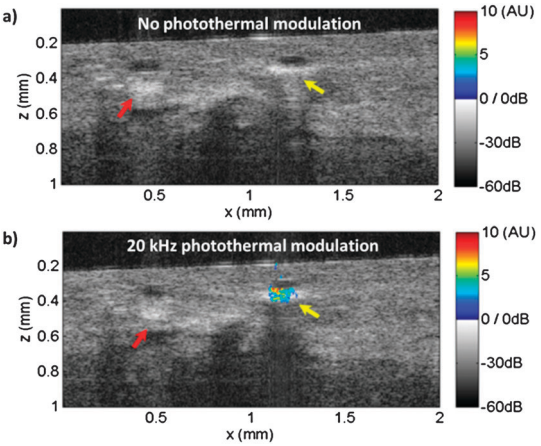

Fig. 4 OCT images with (a) or without (b) photothermal modulation on freshly excised human breast tissue using injected nanorods as contrast agents. Photothermal OCT signal (in arbitrary units) with a SNR > 5 is superimposed as pseudocolor on the gray scale OCT structural image. The yellow arrow indicates the injection site of the nanorods, while the red arrow indicates fibrostromal regions with strong backscattering.

formation of linear gold chains with a high degree of crosslinking and only TPB absorption, whereas the overnight aged $AuCl_4^-$ solution with $Au(OH)_4^-$ species favors the formation of nanorods with both TPB and LPB absorption. Au–Cl species can be reduced faster than $Au(OH)_4^-$,[17] which promotes the fast addition of gold colloids to the linear chains and high crosslinking. In contrast, the slow reduction of $Au(OH)_4^-$ promotes kinetic control of gold addition and rod shape formation.

Optical coherence tomography (OCT) is an emerging biomedical imaging tool for assessing tissue architectural morphology in three-dimensions with resolutions approaching that of standard histopathology.[18] Contrast in conventional OCT is derived from endogenous optical scattering changes within the tissue. Recently, there has been an increased interest in using exogenous contrast agents, such as gold nanoparticles, for OCT applications.[19] Fig. 4 shows cross-sectional OCT images of the human breast tissue in gray scale with the photothermal OCT signal superimposed as pseudocolor (see ESI for further details). In the control experiment, where the 830 nm photothermal modulation beam was turned off, an increased scattering signal was observed at the nanorod injection site (yellow arrow). The increased scattering signal due to the nanorods, however, is indistinguishable from intrinsic scattering variations from stromal tissues in the breast (red arrow). In addition, no photothermal signal was observed (Fig. 4a). When a 20 kHz, 11 mW photothermal beam is applied to the tissue, localized photothermal signal was clearly observed at the nanorods injection site (Fig. 4b). Here, a SNR threshold of 5 was selected to highlight the regions of interest where nanorods were injected. A maximum SNR of 29 was achieved with the 20 kHz photothermal modulation.

These results demonstrate the feasibility of using gold nanorods synthesized in continuous flow with lysine, as the contrast agent for photothermal OCT. This work not only advances the synthesis approaches to obtain biocompatible nanomaterials, but also provides a potential application of using them to register 3D morphological and pathological state of tissues with micro scale resolution. Since the lysine molecules have amine and acid groups simultaneously, they would have potential to specifically bind to DNAs, proteins and other biomolecules.

Authors acknowledge US NSF grant (CHE-0714189, K.F.J.), NIH grants (R01-CA75289-15, J.G.F. and K99-EB010071-01A1, C.Z.) and Air Force Office of Scientific Research contract (FA9550-10-1-0063, J.G.F.) for funding this research. V.S. acknowledges the support of the Fulbright Commission and the Ministry of Education in Spain and M.K. acknowledges the support from Deutsche Forschungsgesellschaft (DFG-GSC80-SAOT)

Notes and references

1 X. H. Huang, I. H. El-Sayed, W. Qian and M. A. El-Sayed, *J. Am. Chem. Soc.*, 2006, **128**, 2115–2120.
2 C. J. Murphy, A. M. Gole, S. E. Hunyadi, J. W. Stone, P. N. Sisco, A. Alkilany, B. E. Kinard and P. Hankins, *Chem. Commun.*, 2008, 544–557.
3 N. R. Jana, L. Gearheart and C. J. Murphy, *J. Phys. Chem. B*, 2001, **105**, 4065–4067.
4 T. Niidome, M. Yamagata, Y. Okamoto, Y. Akiyama, H. Takahashi, T. Kawano, Y. Katayama and Y. Niidome, *J. Controlled Release*, 2006, **114**, 343–347.
5 E. E. Connor, J. Mwamuka, A. Gole, C. J. Murphy and M. D. Wyatt, *Small*, 2005, **1**, 325–327.
6 A. P. Leonov, J. W. Zheng, J. D. Clogston and S. T. Stern, A. K. Patri and A. Wei., *ACS Nano*, 2008, **2**, 2481–2488.
7 M. Z. Liu and P. Guyot-Sionnest, *J. Phys. Chem. B*, 2005, **109**, 22192–22200.
8 C. J. Orendorff and C. J. Murphy, *J. Phys. Chem. B*, 2006, **110**, 3990–3994.
9 O. Bar-Ilan, R. M. Albrecht, V. E. Fako and D. Y. Furgeson, *Small*, 2009, **5**, 1897–1910.
10 S. Koeppl, C. Solenthaler, W. Caseri and R. Spolenak, *J. Nanomater.*, 2011, 515049.
11 X. C. Jiang and M. P. Pileni, *Colloids Surf., A*, 2007, **295**, 228–232.
12 R. Shukla, V. Bansal, M. Chaudhary, A. Basu, R. R. Bhonde and M. Sastry, *Langmuir*, 2005, **21**, 10644–10654.
13 Z. Y. Zhong, J. Z. Luo, T. P. Ang, J. Highfield, J. Y. Lin and A. Gedanken, *J. Phys. Chem. B*, 2004, **108**, 18119–18123.
14 S. Marre and K. F. Jensen, *Chem. Soc. Rev.*, 2010, **39**, 1183–1202.
15 A. Halder and N. Ravishankar, *Adv. Mater.*, 2007, **19**, 1854.
16 Z. L. Wang, M. B. Mohamed, S. Link and M. A. El-Sayed, *Surf. Sci.*, 1999, **440**, L809–L814.
17 J. C. Y. Kah, N. Phonthammachai, R. C. Y. Wan, J. Song, T. White, S. Mhaisalkar, I. Ahmad, C. Sheppard and M. Olivo, *Gold Bull.*, 2008, **41**, 23–36.
18 D. Huang, E. A. Swanson, C. P. Lin, J. S. Schuman, W. G. Stinson, W. Chang, M. R. Hee, T. Flotte, K. Gregory, C. A. Puliafito and J. G. Fujimoto, *Science*, 1991, **254**, 1178–1181.
19 C. Zhou, T.-H. Tsai, D. C. Adler, H.-C. Lee, D. W. Cohen, A. Mondelblatt, Y. H. Wang, J. L. Connolly and J. G. Fujimoto, *Opt. Lett.*, 2010, **35**, 700–702.

